Characterization of the IPG6-B and its Diagnostics

Joshua Edgren, Kathryn Clements, Michael Dropmann, René Laufer, Truell Hyde, and Lorin Matthews

***Abstract*—The Inductively heated plasma generator (IPG6B) at the Center for Astrophysics, Space Physics, and Engineering Research (CASPER) at Baylor University provides valuable insight into the nature of high-enthalpy plasma flows in Helium, argon, and nitrogen. The device and its diagnostics have yet to be characterized. In order for the device to be useful for reentry simulations or for fusion reactor materials testing, a thorough map of its behavior at a wide range of pressures and gas flows were to investigated. For this reason various experiments have been performed with a cavity calorimeter in order to determine the plasma power at distinct parameters.**

Although there is considerable work yet to do, the results have demonstrated trends in the devices behavior which will allow optimal operating conditions to be inferred. Additionally over the course of the analysis of these experiments, a Matlab algorithm was written to isolate stable regions of data and extrapolate equilibrium values and time constants from them. This quantifies the time required for experimental measurements to reach equilibrium after experimental parameters have been changed.

Index Terms—Inductively coupled plasma source, technical plasma,

I. Introduction

THE study of plasma, the fourth aggregate state of matter, has vast implications. The majority of the observable universe consists of plasma; this is seen e.g. in stars, the interstellar medium, and magnetospheres[1]. Furthermore plasma has particular interest to the engineering of spacecraft, as any vessel entering a moon's or a planet's atmosphere will encounter substantial heat fluxes due to the plasma created due to the deceleration in the atmosphere.. Additionally, the magnetic manipulation of plasma is the prevailing method for creating the circumstances required for nuclear fusion to occur. For all these reasons, and for others such as lunar and planetary exploration[2], it is in the interest of physicists to investigate the behavior of this substance.

In collaboration with the Institute of Space Systems (IRS) at the University of Stuttgart, the Center for Astrophysics, Space Physics, and Engineering Research (CASPER) at Baylor University an inductively heated plasma generator test facility was constructed. It allows investigation of plasma at energy levels and of gas mixtures which the Gaseous Electronic Conference (GEC) reference cells cannot sustain[3]. The electrodeless aspect of this device also allows it to safely investigate the plasma of chemically reactive gases.

II. Experimental set-up

The inductively heated plasma generator (IPG6B) at CASPER is the latest plasma wind tunnel in the IPG class, the previous five devices in this class, along with the IPG6S model were developed at the University of Stuttgart, and this seventh device represents a collaborative effort between CASPER and the University of Stuttgart. The IPG6-B is a smaller and lower powered setup than its predecessors IPG3-IPG5 and thus less complex and more cost effective to operate[3]. Though the entire device is commonly referred to as an IPG, the plasma generator itself is actually one of six subsytems which make up the whole setup which would be more accurately called a plasma wind tunnel (PWT). These will be discussed in detail in the subsequent paragraphs.

Fig 1 IPG6-B Vacuum Chamber

A) Elements of the IPG

1) The IPG: Two common but fundamentally different plasma generator concepts are arc jets and inductively coupled generators respectively [4]. Both have essentially the same function: heating the test gas to the point where the kinetic energy of the free electrons exceeds the ionization energy and the gas now consists of a mixture of free electrons and ions we refer to as plasma. In an arc jet the gas is heated by means of

Manuscript received August 5, 2015. This work was supported by the National Science Foundation under grant PHY-1262031

Joshua Edgren is an undergraduate physics student at Union University, Jackson, TN, 38305, USA (email: josh.edgren@gmail.com)

Kathryn Clements is an undergraduate aerospace engineering student at St. Louis University, St. Louis, MO, 63103, USA (email: clementsk@slu.edu)

Michael Dropmann is with the Center for Astrophysics, Space Physics, and Engineering Research, Baylor University, Waco, TX, 76798, USA, and the Institute of Space Systems, University of Stuttgart, 70569 Stuttgart Germany (email: Michael_Dropmann@baylor.edu)

Truell Hyde, Rene Laufer, and Lorin Matthews are with the Center for Astrophysics, Space Physics, and Engineering Research, Baylor University, Waco, TX, 76798, USA. (email: Truell_Hyde@baylor.edu)

an electric arc, while an inductively coupled generator employs an electrodeless inductive heating process. It essentially operates in the same manner as a transformer [3] wherein a high-frequency alternating current is fed into a coil, and this induces an azimuthal electric field by means of an oscillating magnetic field. This electric field induces a voltage in a secondary coil surrounding the azimuthal electric field. In a transformer this effect is used to transfer, increase, or decrease alternating current between two or more circuits. In an IPG the secondary coil is not another circuit, but rather the plasma acts as a secondary coil inside the primary coil. It is the induced azimuthal field which heats the free electrons and ionizes the gas.

The IPG6B operates at power levels of up to 15kW (though the experiments in this paper were conducted at power levels not exceeding 5kW) and a frequency of 13.56MHz [3]. This frequency is specified by U.S. federal regulations. The device is approximately 230mm in length and 130mm in diameter. It consists of an internally water-cooled coil 80mm in length made of 5.5 turns of 8mm copper tubing [3]. This coil surrounds a quartz tube which contains the plasma. Studies by Nawaz and Herdrich have demonstrated that a smaller wall thickness of the quartz tube both increases the efficiency and decreases the thermo-mechanical tensions[5]. Both the coil and the quartz tube are contained in a delrin case which can cope with the high heat loads and thermal stresses present when the device is in operation due to internal water cooling.

2) Vacuum Chamber and Pump: The IPG is mounted inside a Faraday cage on one end of a cylindrical vacuum chamber 2 m in length and 1 m in diameter[3]. At the other end is the valve which connects the chamber to the vacuum pump. This set up allows for a symmetrical plasma flow from one end of the chamber to the other. The vacuum system employed here consists of a rotary vane pump combined with a roots pump which provides a total pumping speed of 160 m^3/h [3]. Additionally a butterfly valve allows the pressure to be regulated to a precision of 0.133 Pa (1 mTorr).

3) Gas Flow Controller: In the end of the case containing the IPG coil the gas is injected through two opposed ports. This injection mode causes the gas to follow a circular path as it enters the discharge channel, and thus it is stabilized as the voltage is induced in it. The gas is supplied by a flow controller which allows the flow of the gas to be regulated. It has a maximum flow of approximately 17.3 std liters/min (SLM). The gases used in the course of these experiments were Helium, Argon, and Nitrogen.

4) Water Cooling system: There are two water systems used in cooling the IPG and the diagnostics; one is medium temperature (MT) water provided by the building's water supply, and the other is deionized (DI) water used to cool the IPG case and coil. The advantage of the DI water is that it is non-conductive and suppresses shorts between the coil's turns. The DI water is cooled by the MT water using a heat exchanger. Additionally the DI water has a chilling unit with the pump and water circulates through the system.[3] The medium temperature water is not chilled and when water has passed through the cooling tubes, it is returned to the building's supply.

5) RF Power Supply & Tuning Network: The radio-frequency generator of the IPG6B is capable of emitting power levels up to 15kW (which is fairly modest for devices of this nature) at a frequency of 13.56 MHz. In the course of the experiments thus far the device has not been operated at a power greater than 5kW. Additionally there is a tuning network which matches the impedance of the circuit and allows for both optimal induced voltage in the plasma while also protecting the power supply from a large reflected power.

A. Diagnostics:

1) Cavity Calorimeter: To determine the power of the plasma at various operating conditions, a cavity calorimeter was employed. This device is conical in shape and consists of water flowing through a continuous copper tube surrounding a cavity and through a helix shaped portion of the tube inside the cavity. The diagnostic is positioned so that the plasma flows directly into the cavity and the thermal energy of the plasma is transferred to the cooling water in the tubing. The temperature of the water is measured as it enters the device and as it exits and this information along with the flow rate and the specific heat capacity of water allows the power of the plasma to be calculated from the equation

Fig 2 Calorimeter in operation

$$P_{cal} = (c_{pwater})(\rho_{water})\dot{V}(T_{out} - T_{in}) \qquad (\mathbf{1})$$

Where c_{pwater} is the specific heat capacity of water in J/kg, ρ_{water} is the density of water in kg/m^3, $\dot{V}$ is the volume flow of the water in m^3/s, and $T_{out} - T_{in}$ is the temperature difference of the calorimeter water return and the water supply in K. This same equation can also be used to calculate the heat losses from the IPG case and coil by simply substituting the specific $\dot{V}$ and $T_{out} - T_{in}$.

Some of the power in the plasma will necessarily escape out the end of the cavity, but this residual thermal and kinetic energy has a specific value for specific operating

conditions[1].

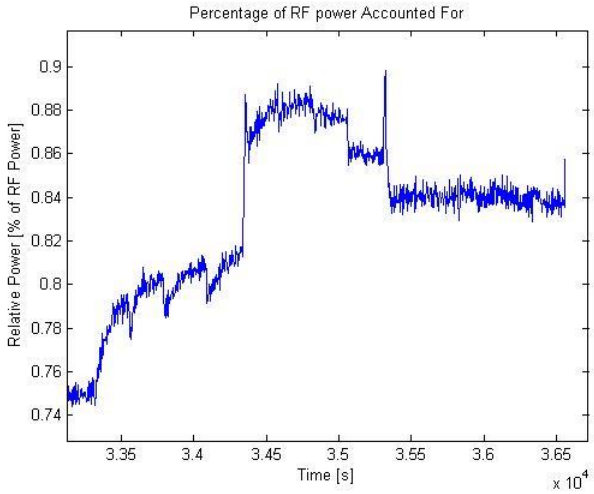

Fig. 3 The sum of the heat losses from the calorimeter and the water cooling the IPG divided by the RF power.

For every set of parameters there is unaccounted power, but much of it is likely thermal losses to the chamber which are not quantified. Since the accounted power is for some operating conditions 90% of the RF power, it can be inferred that the power of the escaped plasma is minimal.

2) Pitot Probe: This device measures the total pressure of the system by introducing a tube into a flowing medium parallel to the stream lines. The medium will flow around the obstacle, but at some point the flow will have been decelerated to zero—called the stagnation point. The pressure at this point is the total pressure of the flow[6]. This value along with the pressure of the vacuum chamber allows the Mach number of the flow to be determined. During experiments conducted here, the Pitot probe is positioned parallel directly on the central axis of the plasma flow.

B. Procedure:

All of the experiments referenced in this paper involved the calorimeter, but in each case a different gas was tested. The goal was to test a wide variety of operating parameters so as to have a thorough understanding of the IPG6B's behavior. When the device is used for active research either in reentry simulation or in investigating the conditions in the diverter region of fusion reactors, Helium or air will be used, but in these experiments both Argon and Nitrogen were tested as well. The gases behave similarly enough to each other that the testing of Ar and N_2 is useful.

In testing the diagnostics of the IPG6-B the objective is to have a map of the device's behavior at a wide range of operating parameters. The three specific parameters investigated were the pressure of the chamber, the gas flow rate, and the distance the calorimeter was from the flange of the IPG where the plasma was emitted. In all cases the item of greatest interest was the power of the plasma as measured by the calorimeter and also the relative power of the plasma for a given RF power, but for all the experiments referenced here the RF power was kept constant. When the experiments are conducted where the RF power is varied, the relative power of the plasma will be of higher importance.

Though the power of the plasma was the item of greatest consideration, an additional anomaly that was investigated was a temperature difference between the temperature sensors located on the flange of the IPG itself. These sensors are located approximately 10 cm apart, yet during certain experiments a 25 degree Celsius temperature difference could be observed between them. This was evident primarily in the Helium experiments. It was observed only under certain conditions, and it seems to be caused by electric discharge induced by the proximity of the calorimeter, but no firm conclusions have been drawn.

III. Experimentation and Data

In the course of the data collection there were primarily three experiments conducted. First, observing Helium plasma over a wide range of pressures; second, observing Nitrogen at a wide range of gas flows (Nitrogen's affordability makes the higher gas flows practical), and third observing Argon at low pressures (due to arcing in the chamber and IPG, these experiments were aborted early). In each of these experiments the RF power was kept at a constant 4kW, and the diagnostic employed was the cavity calorimeter, and thus the item of interest was the power of the plasma as determined by the heat transferred to the calorimeter. This was calculated from equation (1).

A) Helium at various pressures:

In the course of these data collections three parameters were varied: the calorimeter distance, the gas flow, and the pressure of the vacuum chamber. As expected, decreasing the distance between the calorimeter and the flange of the IPG caused greater calorimeter powers to be observed, for this allowed more of the plasma to enter the cavity of the calorimeter. This effect can be seen clearly in fig. 4.

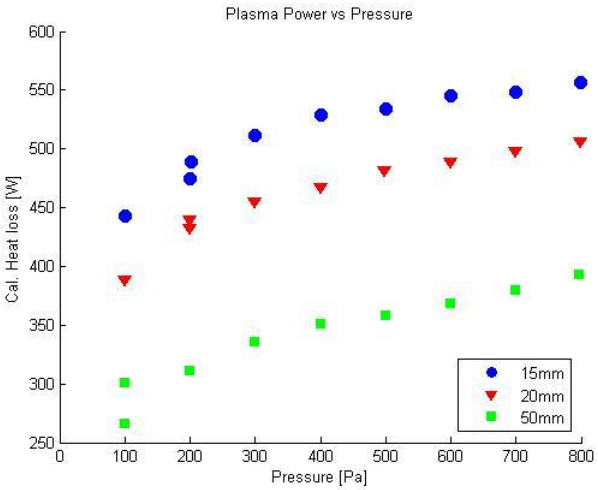

Fig. 4 Plasma power as a function of vacuum chamber pressure for three different runs at a calorimeter distance of 15mm, 20mm, and 50mm respectively

In each of these runs the gas flow was kept constant at 1.0 SLM, and the pressure was increased in 100 Pa increments. From this plot it can also be concluded that the plasma power increases with an increase in pressure, at least over the range used here. This is further evidenced in fig. 5 which shows the plasma power as a function of pressure, but this time for a fixed calorimeter distance.

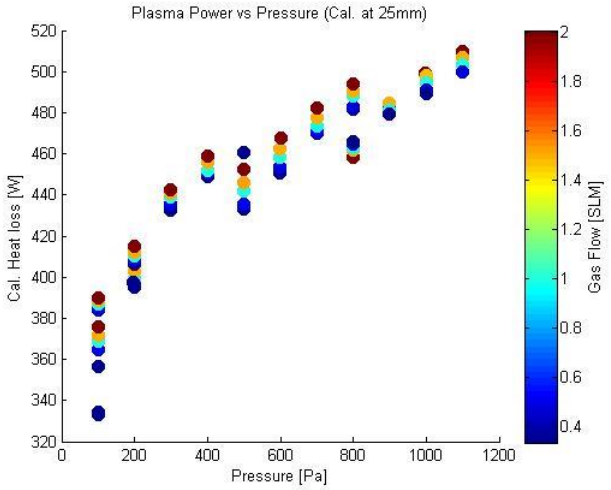

Fig. 5 Plasma Power as a function of vacuum chamber pressure for a constant calorimeter distance of 25mm. The color of each point describes the gas flow at that point.

This plot represents three different days of data collection; this is why there are overlaps and discontinuities. The chamber heats up over the course of data collection, and this affects the power observed in the calorimeter. The data taken at 400 Pa was at the end of a run, when the chamber was hot, and the data taken at 500 Pa was at the beginning of a run when the chamber was still heating up. This is why there is a dip in the trend. Additionally from this graph it can be observed that higher gas flows, at least in the range depicted here, yield higher plasma powers. A noteworthy exception to this trend occurs at 800 Pa where the reverse seems to be true. The data collected in this run, and in the runs at higher pressures, was obtained by beginning at a high gas flow and decreasing in steps rather than all the previous runs where the gas flow was increased in steps. Thus, as the 800 Pa run was at the beginning of an experiment, directly following the warm-up procedure, the decreasing gas flow seemed to increase the heat loss only because the chamber was still reaching an equilibrium. The subsequent three runs return to the previous trend.

A further item of interest here is not only the behavior of the calorimeter power, but also the IPG heat loss. This is measured in the same way as the calorimeter, but it is the temperature difference and flow rate of the water cooling the IPG case and coil that determines the heat loss. This value represents thermal losses in the device. It is lost thermal energy that is not transmitted to the plasma. Fig. 6 is a plot of the IPG heat losses for the same conditions as Fig. 4.

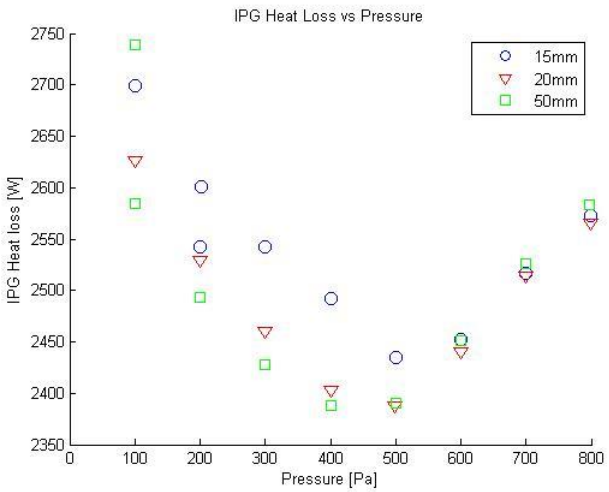

Fig. 6 IPG heat loss as a function of pressure for calorimeter distances of 15mm, 20mm, and 50mm respectively.

While in fig. 4 the plasma power increased as pressure increased, the IPG heat losses decrease to a minimum and then increase again. One would anticipate that as the plasma power increased, the IPG heat loss would decrease, and that is true for a certain range of pressures, but not for all. It seems that at500 Pa some transition occurs which causes the IPG to retain more heat than previously. 500 Pa was also the pressure at which the most plasma instabilities such as sparks and arcing were observed. At 300-400 Pa, sparking in the chamber on the rails above and below the flange could be observed. These effects increased as the pressure was increased to 500 Pa, and at this pressure there were several severe arcs in the chamber. It is likely that these two items are linked: that the greater conductivity of the plasma at certain pressures results in a smaller heat loss in the IPG case and coil.

Another element of interest is that, for certain pressures, a decrease in calorimeter distance results in a greater IPG heat loss. This is consistent for pressures of 100-400 Pa, but again, at 500 Pa a transition occurs and this is reversed. At higher pressures the distance of the calorimeter seems to affect the IPG heat loss only slightly, but the trend is the opposite of what it previously was: the greater calorimeter distance results in a greater IPG heat loss. This could be attributed to small capacitive discharges between the IPG and the calorimeter, but this could not be conclusively stated.

B) Nitrogen at various gas flows:

Due to the affordability of Nitrogen, experiments with much higher gas flows were practical. The cost of Helium made it more reasonable to keep the gas flows in the 0.35-2.0 SLM range, but with Nitrogen this limitation was no longer necessary. Fig. 7 depicts five different calorimeter distances and the plasma power as a function of gas flow for each of them. In the first of these experiments the calorimeter was so far back as to be, it was thought, almost negligible, but at the higher gas flows significant heat losses were observed, so the data set was considered along with the others.

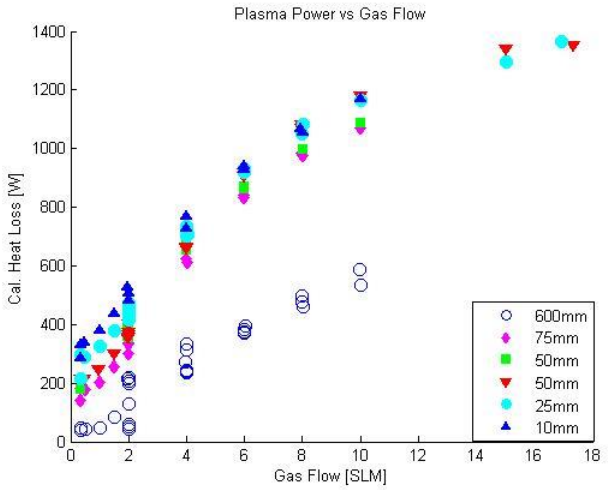

Fig. 7 plasma power as a function of gas flow for five different calorimeter distances: 600 mm, 75 mm, 50 mm, 25 mm, and 10 mm respectively.

Here it is evident that the much higher gas flows result in dramatically higher plasma powers than were observed in the pressure experiments with Helium. It is interesting to note that the maximum plasma powers achieved in the pressure experiments with Helium are comparable to those observed in the 600 mm run at high gas flows. The 600 mm run was originally merely a test to see how the device would respond to gas flows of up to 10 SLM, but the heat losses in the calorimeter were substantial enough to make it worth considering. This fact and the high heat losses registered during the 75 mm run compared to the other runs indicates that the higher gas flows are resulting in a longer plasma jet which makes the position of the calorimeter (and in the future the position of a material sample) less of a factor in considering the power output.

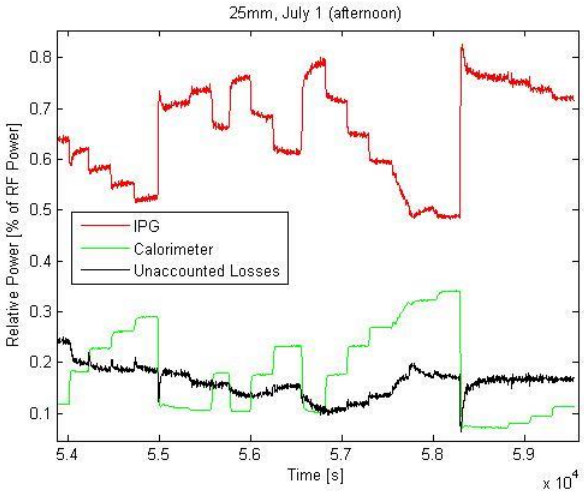

Fig. 8 The relative heat losses of the plasma and the IPG plotted as a function of time for a single experiment with a calorimeter distance of 25mm. Also in black is the difference between the RF power and the sum of the heat losses. This represents unaccounted power losses.

In fig. 8 the power of the plasma and the IPG heat losses are divided by the RF power at each given point. Since the RF power was kept constant at 4kW, this is a simple scaling of the plot of the heat losses, but it indicates the percentage of the total 4kW which is present in the plasma. In this graph it may be observed that at the highest gas flows 34% of the total power was present in the plasma. Compared to the highest value achieved with Helium (12.6%) this is noteworthy. The relative heat losses at the lower gas flows were also quite comparable to those observed in the Helium experiments. This suggests that Helium plasma at higher gas flows would yield similar relative heat losses in the calorimeter. Additionally, the point of highest calorimeter heat loss is also the point of lowest IPG heat loss meaning that the RF power is being converted to plasma power more efficiently at higher gas flows. However, upon examination of the other parameters, it was observed that the unaccounted power losses are also greatest at the higher gas flows. So while more of the RF power which was previously lost in the IPG case and coil is being transferred to the plasma at the higher gas flows, also more of the RF power is being lost elsewhere. Much of it is lost in heating the vacuum chamber, which is not water cooled and thus not quantified, but if we examine plots of the temperature sensor on the chamber for this same run, the temperature of the chamber is highest when the unaccounted losses are highest.

C) *Conductive properties of Argon*

The experiments with argon were curtailed due to the unforeseen electrical phenomena that ensued. There had been some sparking and electrical discharges at certain pressures during the Helium experiments, but the arcs observed with the Argon plasma were considerably more dramatic. There were also plasmoids observed moving between the flange and the rails in the chamber[7], [8]. Due to these arcs and the risk of damage to the IPG, the Argon experiments were not continued. However, it is worth noting that the arcs with the argon plasma were accompanied by spikes in the calorimeter heat loss with severity that corresponded to that of the arc. In previous Helium arcs the IPG heat loss spiked while the calorimeter heat loss dipped. With Argon, both spiked. Thus during this arc, RF power that is usually not transmitted to either the calorimeter or to the IPG was diverted.

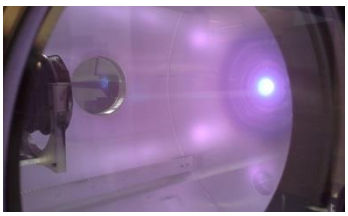

Fig 9 Plasmoids in Argon plasma

IV. Data Analysis

The data from all the sensors employed in the IPG is fed into Labview where it can be monitored during experimentation. When the experiments are complete, the raw data (level-0) is saved. It is then further post processed and heat losses are calculated based on the raw data. This data is defined as level-2 data. Fig. 8 is an example of level-2 data.

This data gives all experiment parameters as functions of the time of the experiment. As a next step, stable data points (regions of a minimum length of 100 s where the pressure, gas flow, and power change less than a defined threshold) are identified and average values across these regions are calculated. This data is defined as level-3-data. Fig. 4-7 are examples of level3_data. This allows parameters to be plotted as functions of each other allowing identification of dependencies between parameters.

As part of this project a new data level (level-4-data) has been defined. Level-4 data is generated based on the level-2 data and extrapolates a predicted equilibrium value for a region as measured values have not necessarily reached equilibrium in the experiment time. Fig. 10 depicts temperature sensor data which do not appear to reach an equilibrium value over the allotted time interval.

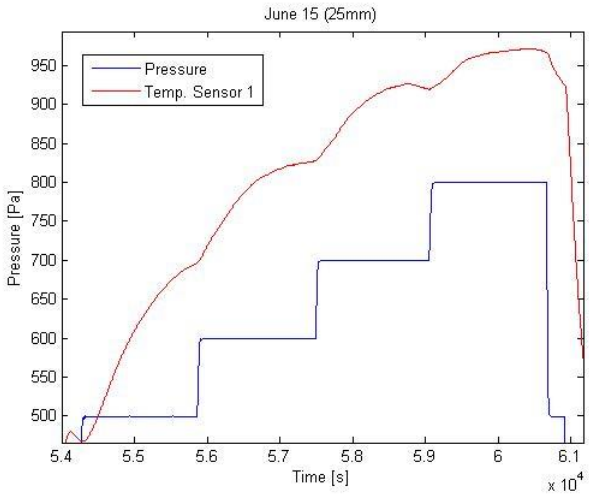

Fig. 10 Changes in pressure over time and the resultant changes in temperature. The temperature data has been scaled to fit on this graph and is depicted here only to show trends.

The idea behind the level-4 data class is to take every stable region (as defined by the level-3 data function) and fit an exponential function to it of the form

$$f(x) = a + be^{cx} \qquad (\mathbf{2})$$

to the region. From this fit the coefficients can be taken and the equilibrium value can be obtained from the value of 'a'. Additionally the coefficient 'c' can be taken and gives the time constant for this equilibrium value. The inverse of the time constant gives the time needed for the system to reach 1-1/e of the expected equilibrium value. Thus if the time constant coefficient is 0.01, after 100 s, the system will be at approximately 0.63 of its equilibrium. After another 100 s the system will be at 0.86 of its equilibrium value. After another 100 s it will be at 0.95 of its equilibrium value, and so on. Thus after 300 s, the system will be close to equilibrium.

In order to quantify the time needed for various parameters to reach an equilibrium, this level-4 data was needed. Once the code was written, the time constants for every stable region of every parameter could be easily accessed. Histograms of these values depict the spread of time constant values which shows the average time it takes for each parameter to come to equilibrium. Fig. 11 and fig. 12 are two such histograms.

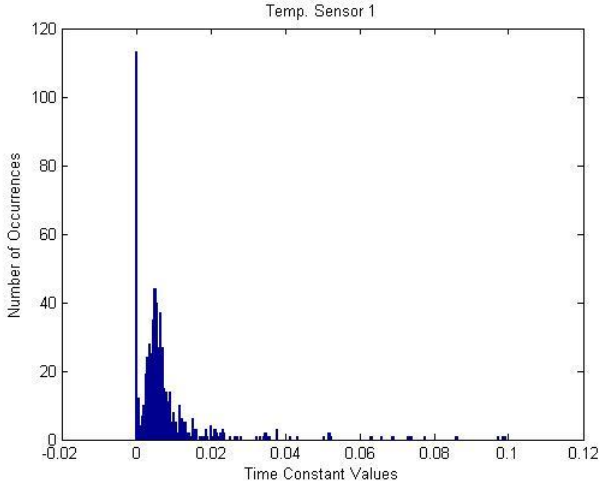

Fig. 11 Histogram of the time constant values for temperature sensor 1 which is on the flange of the IPG.

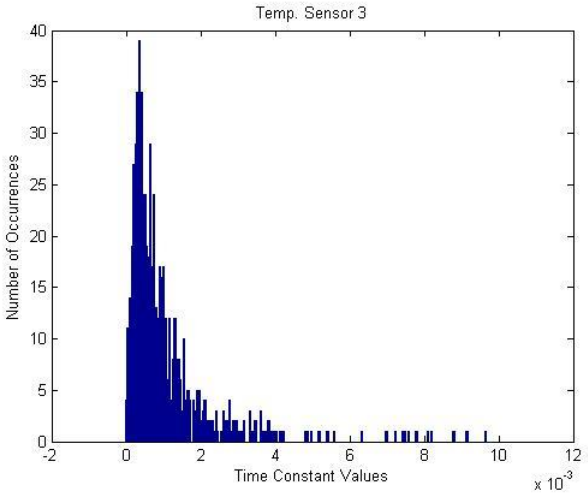

Fig. 12 Histogram of the time constant values for temperature sensor 3 which is on the outside of the IPG vacuum chamber.

The peaks in these graphs depict the most common time constant values for the given parameter. The peak for sensor 3 (on the outside of the chamber) is shifted to the left of that for sensor 1 (on the flange). Smaller time constants mean longer times to reach equilibrium. The temperature sensor on the flange is subject to a greater variety of heat fluxes and it is closer to the elements which are water-cooled, thus it will come to equilibrium faster than the sensor on the outside of the chamber far from any cooling water. The spike before the peak in fig. 11 could have a one of several explanations but two are most likely: it could be a second peak (technically a 'first peak') which has legitimate physical meaning, or it could be the result of errors in the fitting code. The latter is more likely, and that would make sense why it is not seen in the sensor 3 histogram. For sensor 1 there are many stable regions which nonetheless have irregular changes in temperature. An exponential function will not be a good fit to these, and thus

the coefficients will be unreliable.

V. Conclusions

The results in this paper give a preliminary understanding of the behavior of Helium plasma at a wide range of pressures and of the behavior of nitrogen plasma at a wide range of gas flows. From what has been observed, it may be assumed without gross error that the behavior of nitrogen at high gas flows gives a reasonable prediction of the behavior of Helium under similar conditions. The greater efficiency of the nitrogen plasma at higher gas flows is also worth noting.

Finally, the level-4 data which was generated will aid in quantifying the behavior of the IPG6-B; particularly in determining the optimal length of future data collection runs.

Future work will include continued experiments with the Pitot probe and eventually the heat flux probe. A water-cooled converging nozzle has been designed and constructed for the flange of the IPG so as to achieve supersonic plasma velocities. This will require more experiments to quantify and validate.

VI. Acknowledgment

Firstly, I would like to extend sincerest thanks to Michael Dropmann whose guidance and supervision over this project made the summer a thoroughly enjoyable experience. Secondly, Kate Clements deserves recognition as a worthy comrade whose labors and insights were greatly appreciated, and I am grateful. Additionally, Jimmy Schmoke and Mike Cook were above and beyond helpful, and their training, assistance, and supervision in the CASPER lab were all a blessing. I would like to thank Dr. Lorin Matthews and Lori Scott for advice aptly spoken. I would also like to thank Dr. Rene Laufer for his kind instruction and generosity. And finally, I would like to thank the National Science Foundation which funded this research. And in all things, glory to God.

References

[1] K. Boehm, "Characteristic of the Inductively Heated Plasma Source IPG6-B using Helium." Technische Universitat Dresden, 16-Feb-2015.

[2] G. Herdrich, R. Laufer, M. Dropmann, R. A. Gabrielli, and T. W. Hyde, "Establishing a Hybrid Plasma Environment Simulation Facility," *Front. Aerosp. Eng.*, vol. 1, no. 1, 2012.

[3] M. Dropmann, G. Herdrich, R. Laufer, D. Puckert, H. Fulge, S. Fasoulas, J. Schmoke, M. Cook, and T. W. Hyde, "A new inductively driven plasma generator (IPG6)—Setup and initial experiments," 2013.

[4] M. Auweter-Kurtz, M. Feigl, and M. Winter, "Diagnostic Tools for Plasma Wind Tunnels and Reentry Vehicles at the IRS," Apr. 2000.

[5] A. Nawaz and G. Herdrich, "Impact of plasma tube wall thickness on power coupling in ICP sources," *Plasma Sources Sci. Technol.*, vol. 18, no. 4, p. 045018, Nov. 2009.

[6] M. Schuff, "Development of Measurement Inserts for a Multipurpose Plasma Diagnostic Probe." Institut für Raumfahrtsysteme, Universität Stuttgart, Jan-2015.

[7] D. Go, "Gaseous Ionization and Ion Transport: An Introduction to Gas Discharges," Department of Aerospace and Mechanical Engineering, University of Notre Dame, IN 46556, 2012, pp. 1–45.

[8] M. Mikikian, H. Tawidian, and T. Lecas, "Unstable Plasmoids in Dusty Plasma Experiments," *IEEE Trans. Plasma Sci.*, vol. 42, no. 10, pp. 2670–2671, Oct. 2014.

Joshua Edgren is a student at Union University in Jackson, TN and will receive his B.S. in physics in 2016. He is a member of the Society of Physics Students (SPS) and a part of the Research Experience for Undergraduates program at Baylor University's Center for Astrophysics, Space Physics, and Engineering Research (CASPER). He received the Kyle L. Hathcox Memorial Physics award in 2015 (Union University), and his research interests include plasma facilities, plasma conductivity, and space sciences.

Kathryn Clements was born in Glens Falls, NY in 1995. She will receive the B.S. degree in aerospace engineering from Saint Louis University, St. Louis, MO in 2017. She is currently an Engineer at Saint Louis University's Space Systems Research Lab, St. Louis, MO. Ms. Clements is a member of the Society of Women Engineers. She was a recipient of the Excellence in Mathematics Award (Department of Mathematics and Computer Science, Saint Louis University) in 2014."

Michael Dropmann is research assistant at the Center for Astrophysics, Space Physics and Engineering Research (CASPER), member of the Space Science Lab of CASPER and a Ph.D. candidate at the Institute of Space Systems of the Univ. Stuttgart. He received his diploma in aerospace engineering from Univ. Stuttgart. His research interests include plasma facility design, plasma surface interactions and space sciences.

Rene Laufer is associate research professor at the Center for Astrophysics, Space Physics and Engineering Research (CASPER) and head of the Space Science Lab of CASPER. He was born in Berlin, Germany in 1968 and received his diploma in aerospace engineering from Technical Univ. Berlin and his Ph.D. from Univ. Stuttgart, Germany. He was involved in planetary missions at the DLR-Institute of Space Sensor Technology and Planetary Exploration and later became small satellite project manager and lecturer at the Institute of Space Systems, Univ. Stuttgart. His research interests include small satellites, lunar and planetary exploration, lunar bases, ISRU, dust and plasma, small bodies, remote sensing, systems engineering, education and public outreach.

Truell W. Hyde was born in Lubbock, Texas in 1956. He received the B.S. in physics and mathematics from Southern Nazarene University in l978 and the Ph.D. in theoretical physics from Baylor University in 1988.
He is currently at Baylor University where he is the Director of the Center for Astrophysics, Space Physics and Engineering Research (CASPER), a professor of physics and the Vice Provost for Research for the University. His research interests include space physics, shock physics and waves and nonlinear phenomena in complex (dusty) plasmas.

Lorin Matthews grew up in Paris, Texas, and earned her B.S. and Ph.D. degrees from Baylor University. From 1998-2000 she was employed as an engineer at Raytheon Aircraft Integrations Systems, where her main project was vibroacoustics analysis for NASA's Stratospheric Observatory for Infrared Astronomy (SOFIA). In 2000 she returned to Baylor as a lecturer in the Physics Department and Baylor Interdisciplinary Core and Senior Research Scientist with CASPER (2000-2006), and is now an Associate Professor of Physics and Associate Director of CASPER. With four young children at home, the hobby she most often gets to practice is decorating cakes for birthdays and other special occasions.